Journal of Environmental Health Science and Engineering (2019) 17:701–709
https://doi.org/10.1007/s40201-019-00385-8

RESEARCH ARTICLE

Use of metal-organic framework to remove chromium (VI) from aqueous solutions

Zahra Noraee[1] · Ali Jafari[1] · Mansour Ghaderpoori[1,2] · Bahram Kamarehie[1] · Afshin Ghaderpoury[3]

Received: 24 October 2018 / Accepted: 10 June 2019 / Published online: 18 June 2019

Abstract

Chromium is one of the heavy metals found in industrial wastewaters, which have highly toxic to human beings and the environment. Exposure with it may cause some hazard diseases including stomach ulcers, liver, vomiting, kidney and nerve tissue damage, cancer in the lungs, and eventually death. The main objective of this study was to evaluate the efficiency of Uio-66 and ZIF-8 in removing chromium from aqueous solutions. For the synthesis of Uio-66 and ZIF-8, hydrothermal and sol-gel methods were used, respectively. The prepared Uio-66 and ZIF-8 were identified by FTIR, XRD, FE-SEM, EDX, and BET. All experiments were done in batch conditions. Uio-66 and ZIF-8 efficiency for chromium adsorption from aqueous solutions were investigated by variables like initial concentration (10–200 mg/l), pH (3 to 11), Uio-66 and ZIF-8 dosage (0.2 to 1 g/l) and contact time (45 min). The FE-SEM image showed that the sizes of Uio-66 crystals were between 140 and 280 nm. The specific surface area and total pore volume of the prepared Uio-66 and ZIF-8 were 800 m^2/g, 0.45 m^3/g, 1050 m^2/g, and 0.57 m^3/g, respectively. The results show chromium adsorption has increased in acid conditions. Equilibrium dosage for Uio-66 and ZIF-8 was 0.4 g/l and 0.6 g/l, respectively. Adsorption equilibrium was performed after 60 min and after this time, chromium adsorption did not significantly change. The study results showed that the experimental data obtained fitted with kinetic model pseudo-order-reaction and isotherm model of Langmuir.

Keywords Chromium · Uio-66 · ZIF-8 · Drinking water · Adsorption

Introduction

Heavy metals are the environmental pollutants that human exposure to them through water and food can cause severe chronic and severe poisoning. Drinking water pollution with heavy metals is a serious problem in developing countries. Heavy metals such as lead, copper, cadmium, zinc and nickel are the most common pollutants found in industrial wastewater [1]. Chromium is one of the heavy metals found in industrial wastewaters, which have highly toxic to human beings and the environment [2]. In the environment, chromium ion can exist in hexavalent Cr and trivalent Cr forms with different toxicity. Chromium ion 6 toxicity is greater than 3 (almost 100 times) [3, 4]. The World Health Organization (WHO) has confirmed the carcinogenicity of chromium in humans [5]. The US Environmental Protection Agency (USEPA) and National Iranian Standard (NIS) have set the maximum allowed concentration for chromium in drinking waters 0.1 mg/l (or 100 ppb) and 0.05 mg/l, respectively [6, 7]. Exposure with Cr(VI) may cause some hazard diseases including stomach ulcers, liver, vomiting, kidney and nerve tissue damage, cancer in the lungs, and eventually death [4, 6]. Chromium accumulation in animal and plant tissues can cause serious problems. Cr(VI) is usually present in the effluent in the form of chromite anions (CrO_4^{-2}) and dichromate ($Cr_2O_7^{-2}$), and it does not easily precipitate by conventional methods [8]. So far, different methods have been used to remove chromium such as chemical precipitation, co-agulation and flocculation processes, electrocoagulation, ion exchange, adsorption, bio-sorption, and reverse osmosis [9]. Also, these treatment methods have not been highly effective

✉ Mansour Ghaderpoori
ghaderpoori.m@lums.ac.ir

[1] Department of Environmental Health Engineering, School of Health and Nutrition, Lorestan University of Medical Sciences, Khorramabad, Iran

[2] Nutritional Health Research Center, Lorestan University of Medical Sciences, Khorramabad, Iran

[3] Student Research Committee, Shahid Beheshti University of Medical Sciences, Tehran, Iran

in eliminating heavy metals and also the costs in these methods are very high. Of these, the adsorption process has been considered more by many researchers. Some of its benefits include high efficiency, environmentally friendly, low cost, flexibility, simple design and operation, and cost-effective [6]. In general, adsorption is to keep a substance on the surface of the absorbent or the penetration into the internal absorbent pores [10]. So far, various metal-organic frameworks have been used to remove chromium. Some of these adsorbents are ZIF-67 [11], Uio-66 and Uio-66-NH_2 [12], U-H_4btec MOF [13], a silver-triazolato framework [14], and Cu-BTC [1]. Metal-organic frameworks, MOFs, are a new class of crystalline materials with high porosity and high surface area constructed by metal-containing nodes connected by different organic bridges, which bear multiple complexing functions [15]. MOFs are in two main parts, including organic and inorganic [16]. Compared with the conventional adsorbents, MOF adsorbents present fascinating merits because if their different compositions and structures, such as higher surface area and porosity, greater pore volume, modifiable surface, and tunable pore size [17]. The innovation of this study was the use of a new class of adsorbents to remove chromium from aqueous solutions. According to the literature review, so far, no articles have been published on the use of Uio-66 and ZIF-8 to remove chromium. It should be noted that in 2013, Shen et al. used adsorbents of Uio-66 and Uio-66-NH_2 as an efficient visible-light-driven photocatalyst for selective oxidation of chromium [12]. The new adsorbents have shown a high surface area that makes them suitable to remove different heavy metals. In this study, we report the first adsorptive of Cr (VI) from aqueous solutions with a Uio-66 and ZIF-8 to investigate the possibility of using MOFs as suitable adsorbents for the removal of Cr (VI). Among different adsorbents, University of Oslo 66 (Uio-66) and Zeolitic Imidazole Frameworks (ZIF-8) were selected. UiO-66 contains hexanuclear zirconium clusters linked by terephthalates. This MOF might have favourable interactions, such as π-τ interactions, with Cr (VI) for adsorption [18]. Therefore, the main objective of this study was to evaluate the efficiency of Uio-66 and ZIF-8 in removing chromium from aqueous solutions.

Materials and methods

Materials (Uio-66 and ZIF-8, chromium)

Zirconium chloride, terephthalic acid (TPA) were obtained from Merk Company. Potassium permanganate ($KMnO_4$), N, N-dimethylformamide, Zinc nitrate hexahydrate, 2-methylimidazole, and methanol were prepared by Sigma-Aldrich. All reagents and solvents were used as received from commercial suppliers without further purification.

Synthesis of Uio-66 and ZIF-8

UiO-66 and ZIF-8 were prepared was synthesized based on the previous method [19–21]. For the synthesis of Uio-66, $ZrCl_4$ [22] (1 mmol or 0.2332 g) and TPA (1 mmol or 0.161 g) were dissolved in 50 ml of DMF solution. The mixed solutions were transferred to a 100 ml an autoclave. The autoclave was sealed and heated in an oven at 120 °C for 48 h. After cooling, the final white powder was washed several times with methanol. After washing with methanol, the white powder was dried at 100 °C for 12 h in vacuum conditions. Ultimately, the end powder was stored. For the synthesis of ZIF-8, 2-methylimidazole (11.350 g) and of Zinc nitrate hexahydrate (0.863 g) were dissolved in 8 ml and 80 ml deionized water, respectively. The two solutions were combined under constant stirring at room temperature for 8 h. Then, a white powder formed and that was isolated by centrifuge. Ultimately, the end product was dried 24 h. Before use for activating, ZIF-8 was dried for an overnight at 100 °C in a vacuum oven.

General characterization

The prepared Uio-66 and ZIF-8 were identified by Fourier Transform Infrared spectroscopy spectra (Spectrum two model, PerkinElmer Company), X-Ray Diffraction (X' Pert Pro model, Panalytical Company), Energy Dispersive X-ray Spectroscopy, Field Emission Scanning Electron Microscopy (SIGMA VP-500 model, ZEISS Company), and BET surface area. The total pore volume of the adsorbents was also characterized by using nitrogen adsorption isotherms at 77 K (BElSORP Mini model, Microtrac Bel Corp).

Adsorption studies

Chromium adsorption was studied by Uio-66 and ZIF-8 zeolite imidazole framework. All experiments were done in batch conditions. Uio-66 and ZIF-8 efficiency for chromium adsorption from aqueous solutions were investigated by variables like initial concentration (10–200 mg/l), pH (3 to 11), Uio-66 and ZIF-8 dosage (0.2 to 1 g/l) and contact time (45 min). Method of one point at the time was used to determine the number of samples in this study. In this way, only one variable is considered in each step, and the rest of the variables are assumed to be constant. Finally, to determine the optimum conditions and also to determine the isotherms and kinetics adsorption, 210 samples were examined for both adsorbents (Uio-66 and ZIF-8). Also, each experiment was repeated three times. So, Therefore, the effect of variables in constant time (in this study was 45 min). In the step of determining the adsorption kinetics, the effect of the contact time was more accurately investigated. At first, a stock solution of chromium was made and stored under standard conditions. Potassium dichromate, $K_2Cr_2O_7$, was used to prepare the standard solution (1000 mg/l). An absorbent dosage was added to

100 ml of chromium solution. The solution pH was adjusted using HCl and NaOH (1 N). At the beginning and the end, the adsorbent was isolated from solution by centrifuge (3000 rpm, 5 min). Then, the residual chromium was measured by a spectrophotometer (UV-UVIS) [23]. The residual chromium concentration at 540 nm was determined. In the first step, the calibration curve for chromium was plotted in the range of 0.1 to 0.7 mg/L (R2 = 0.9987, Y = 1.4836 + 0.0699). All experiments were performed at laboratory temperature [24]. Eventually, adsorbed chromium (q_e, mg/g) on the Uio-66 and ZIF-8 was estimated according to Eq. 1 [25–27]:

$$q_e = \frac{V(C_o - C_e)}{m} \quad (1)$$

Where, C_o and C_e are an initial and final concentration of chromium (m/l), respectively, V is the volume of chromium solution (ml), and m is the adsorbent weight (g). Also, the removal efficiency (R, %) of chromium was estimated according to Eq. 2 [28]:

$$R, \% = \frac{(C_0 - C_t)}{C_0} \quad (2)$$

Where, C_o and C_t are the initial and final concentration of chromium (mg/L), respectively. To determine the adsorption isotherms of chromium on Uio-66 and ZIF-8, the models of Langmuir (plotting C_e/q_e against C_e) and Freundlich (plotting log q_e against log C_e) were investigated. To determine the adsorption rate of chromium, the kinetic models of pseudo-first-order (plotting ln푞 −) versus time) and the pseudo-second-order (plotting t/ versus time) were used [4]. the experiments of adsorption equilibrium were investigated at optimal conditions of chromium adsorption [29]. Equilibrium studies were performed at laboratory temperature using 50 ml of chromium with varied initial concentrations (50 mg/l and 60 mg/l).

Data availability Data sharing not applicable to this article as no datasets were generated or analyzed during the current study.

Results and discussion

Characterization of prepared Uio-66 and ZIF-8

The crystallographic structure of prepared Uio-66 and ZIF-8 were studied by X-Ray Diffraction. The XRD patterns and FESEM image of the prepared Uio-66 and ZIF-8 are shown in Fig. 1. As shown in Fig. 1-A, the XRD pattern of the Uio-66 has three clear at 7°, 8.45°, 25.69° [20, 26]. The results of this

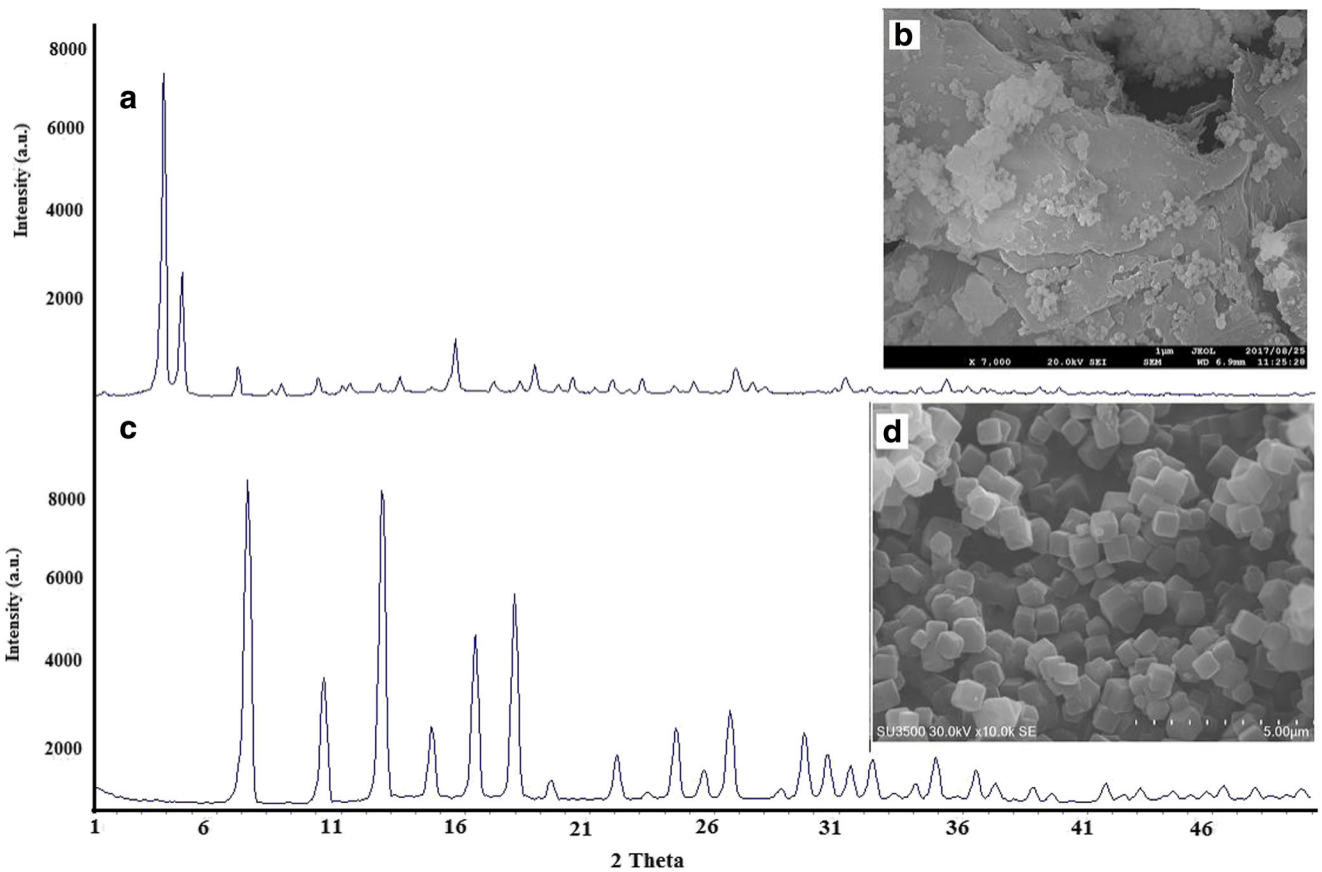

Fig. 1 XRD spectra and FE-SEM image of the prepared Uio-66 (**a, b**) and ZIF-8 (**c, d**)

Table 1 Some properties of Uio-66 and ZIF-8 based on BET

Adsorbent	SA_{BET} ($m^2\ g^{-1}$)	Total pore volume ($m^3\ g^{-1}$)	Mean pore diameter (nm)
Uio-66	800	0.45	2.33
ZIF-8	1050	0.57	1.54

study were consistent with the findings of the other researchers [16, 21, 30, 31]. Figure 1-B shows the morphology of prepared Uio-66. The FE-SEM image showed that the sizes of Uio-66 crystals were between 140 and 280 nm. In Lin study, produced Uio-66 size was between 200 to 500 nm [32]. Some properties of prepared Uio-66 are shown in Table 1. The specific surface area and total pore volume of the prepared Uio-66 was 800 m^2/g and 0.45 m^3/g. In various studies, the specific surface area is slightly different, which can be attributed to the synthesis method and the quality of the materials used. The XRD patterns and FESEM image of the prepared ZIF-8 are shown in Fig. 1-B and 1-C, respectively. As shown in Fig. 1-B, the XRD pattern of the ZIF-8 has peaks at 7°, 10°, 12°, 14°, 16°, and 18°. The spectrum obtained was consistent with other studies. In both the Uio-66 and ZIF-8 in the XRD spectrum, the presence of clear and distinct peaks indicated that the crystallization of MOFs has been well done [33, 34]. Unlike Uio-66, which is almost amorphous, ZIF-8 have different morphologies like cubic, leaf-shaped, and dodecahedral [19]. The results of previous studies showed which the surface area of MOFs can vary depending on morphology, the quality of used materials for synthesis, and finally synthesis conditions. As can be understood from Fig. 1-D, ZIF-8 was synthesized into a cubic shape. As shown in Table 1, the specific surface area and total pore volume of the prepared ZIF-8 was 1050 m^2/g and 0.57 m^3/g. The cube dimensions of prepared cubic ZIF-8 was in the range of between 455 to 760 nm. The perpend ZIF-8 was white powder and its density was 0.45 g/m^3. In the studies Khan et al. and Liu, the reported surface area was 1501 m^2/g and 958.4 m^2/g, respectively [19, 35]. In the study of Liu et al., the surface area of dodecahedral-ZIF-8, cubic-ZIF-8, and leaf-shaped-ZIF-8 also were 1151.2 m^2/g, 958.4 m^2/g, and 12.7 m^2/g, respectively [19]. The results of EDX showed that the percentage of C, N, Zn, and O in the ZIF-8 was 49%, 22%, 27.7%, and 1.54%, respectively.

In the adsorption processes, the solution pH has an important effect on the reaction progression and adsorption capacity. The solution pH affects the distribution of charge on the adsorbent surface and dissociation the target pollutant [36]. Chromium adsorption at different pH was investigated. The effect of solution pH on adsorption of chromium on the Uio-66 and ZIF-8 was investigated over a pH range of 3 to 11 with a contact time of 45 min. Figure 2 shows the adsorption efficiency of chromium with adsorbents Uio-66 and ZIF-8. The selective concentration of chromium for these experiments was 50 mg/l. As shown in Fig. 2, chromium adsorption has increased in acid conditions. The relatively lower pH was favourable for the chromium adsorption. When the solution pH decreased from 11 to 3, the capacity of chromium adsorption on the Uio-66 and ZIF-8 increased from 15.6 to 85.7 mg/g and from 35.4 to 150 mg/g, respectively. According to studies on the distribution of different species of chromium at different pH, its various forms are H_2CrO_4 (chromic acid), $H_2CrO_4^-$ (hydrogen chromate ions), and CrO_4^{-2} (chromate ions). Also, chromic acid and hydrogen chromate ions are the dominant forms when the solution pH is lower than 6.8, while only chromate ions are stable when the pH is above 6.8 [11, 37]. For accurate examination of the chromium adsorption process on adsorbents, pH_{ZPC} was first measured [38]. pH_{ZPC} for Uio-66 and ZIF-8 was obtained 7 and 9, respectively. Therefore, at lower pH than these values, the surface

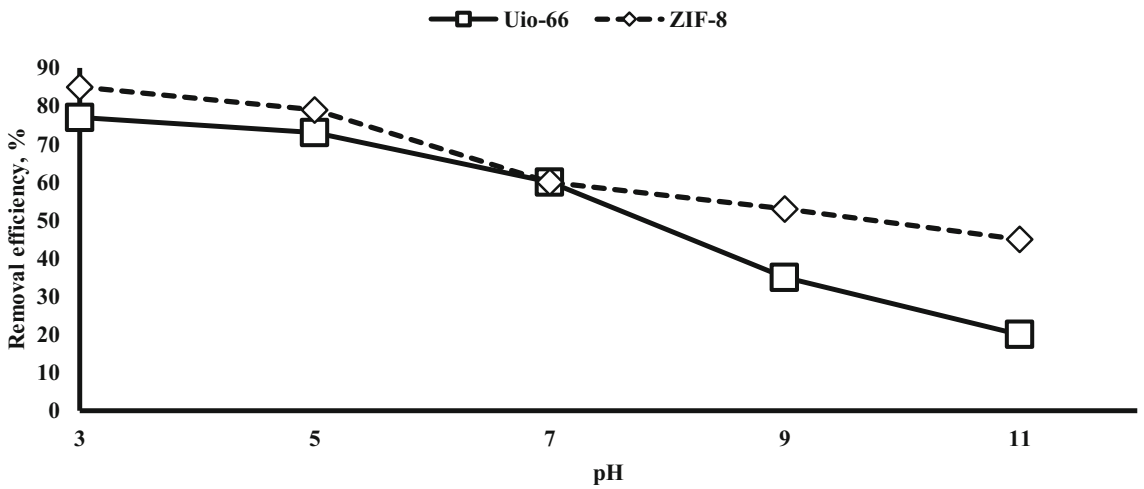

Fig. 2 The pH effect onto chromium (VI) adsorption by Uio-66 and ZIF-8

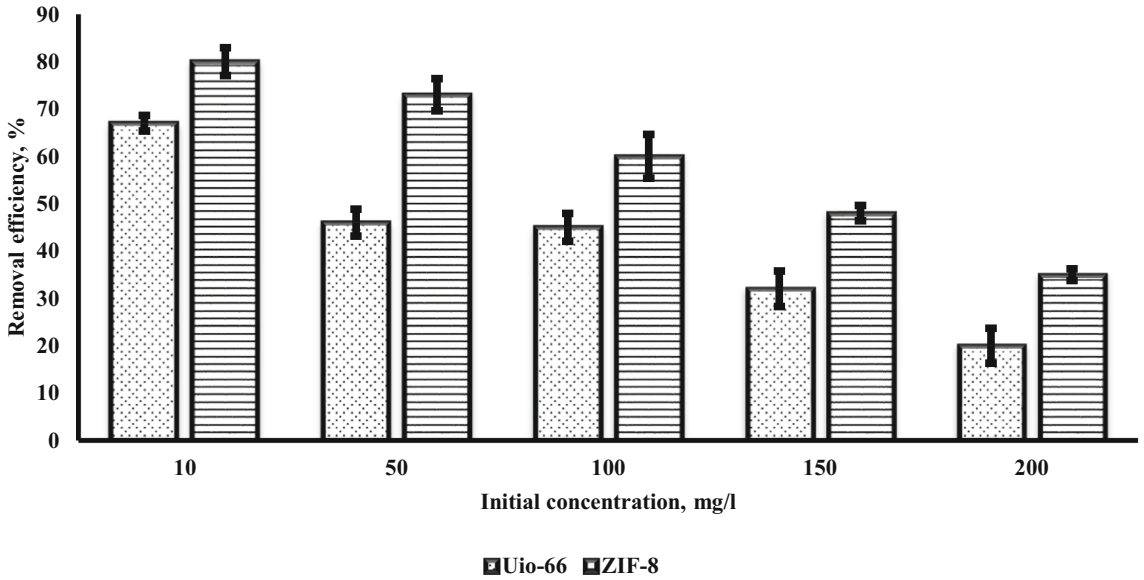

Fig. 3 The effect of initial chromium concentration by Uio-66 and ZIF-8 (pH: 3, contact time: 45 min)

charges of the adsorbents are positive. Consequently, in these conditions, the strong electrostatic interaction of among adsorbents and chromium anions occurs when the solution pH is lower than pH_{ZPC}. Li et al. (2015) reported that ZIF-67 adsorbent has a significant effect on chromium adsorption at acid pH [11]. In this study, when the pH value decreases from 11 to 5, the adsorption capacity of Cr (VI) on the ZIF-67 increases from 3.27 to 13.2 mg/g. The results of this study are consistent with other researchers' findings [11, 39–41]. Maleki et al. (2015) reported that they used Cu-BTC adsorbent to chromium adsorption [1]. Khosravi et al. (2018) reported that the high capacity of chromium adsorption at acidic pH is due to the presence of different forms of Cr(VI) in the solution, including H_2CrO_4, $HCrO_4^-$, CrO_4^{2-}, and $Cr_2O_7^{2-}$ [6]. Mobarak et al. (2018) used CTAB/H_2O_2-clay to remove chromium. The results showed that the highest adsorption capacity was observed at pH ≈ 2. [4]. Based on Khosravi et al. report (2018), Chromium adsorption reactions are as follows [37]:

$$Cr_2O_7^{-2} + H_2O \Rightarrow 2HCrO_4^- \quad (3)$$

$$HCrO_4^- \Rightarrow CrO_4^{-2} + H^+ \quad (4)$$

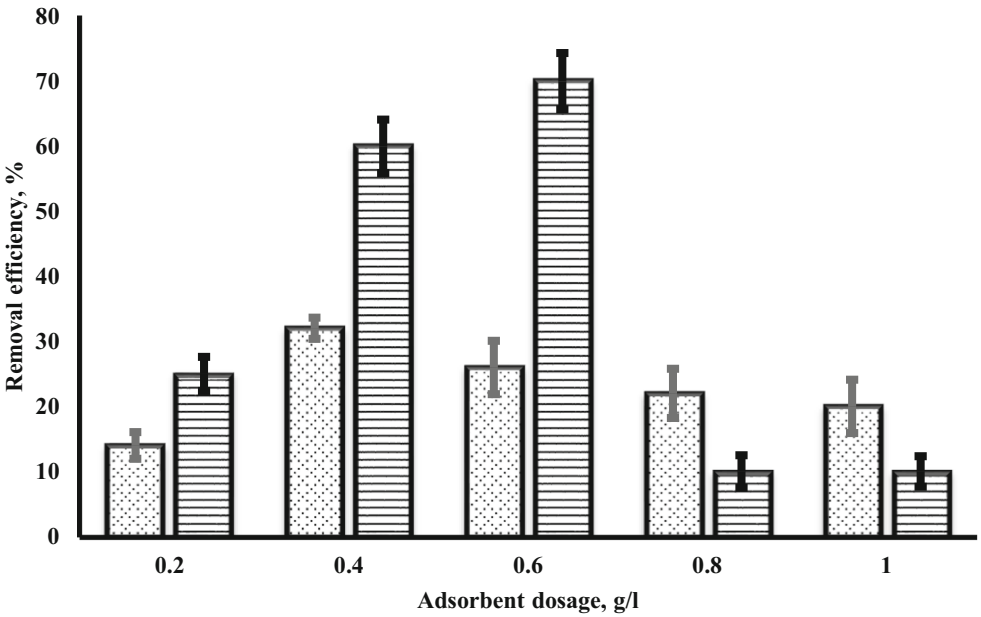

Fig. 4 The effect of adsorbent dose of Uio-66 and ZIF-8 onto chromium adsorption (pH: 3, contact time: 45 min, and initial concentration: 50 mg/l)

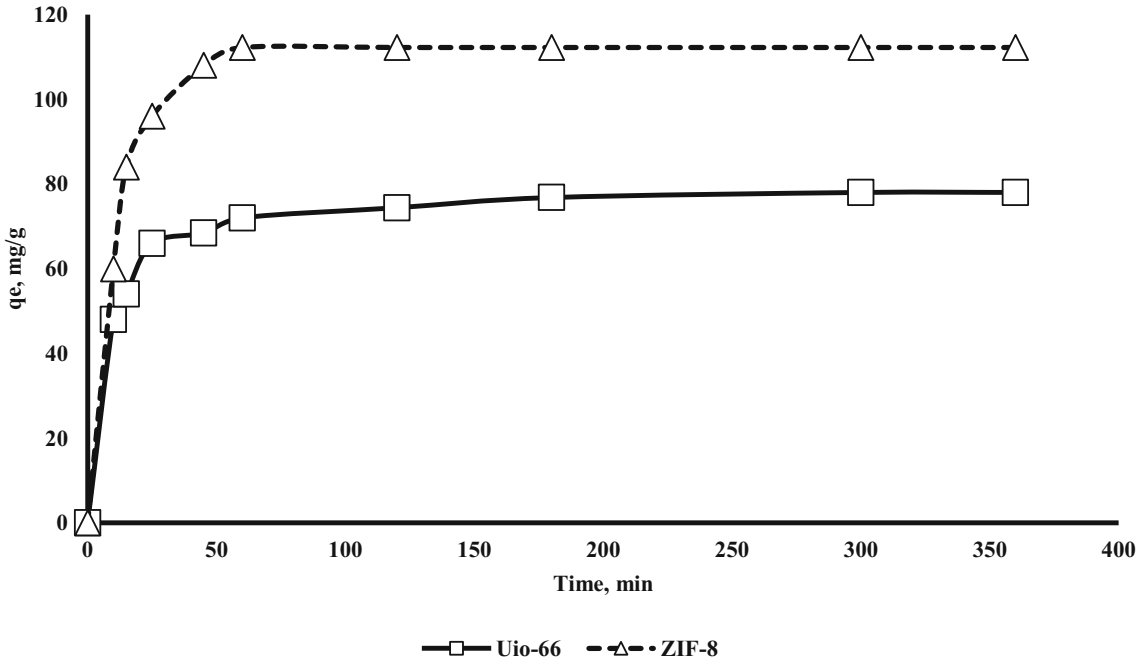

Fig. 5 Effect of contact time on chromium adsorption onto Uio-66 and ZIF-8

$$HCrO_4^- + 7H^+ + 3e^- \Rightarrow 4H_2O \quad (5)$$

$$CrO_4^{-2} + 14H^+ + 6e^- \Rightarrow 2Cr^{3+} + 7H_2O \quad (6)$$

$$Cr_2O_7^{-2} + 14H^+ + 6e^- \Rightarrow 2Cr^{3+} + 7H_2O \quad (7)$$

In alkaline conditions, the concentration of hydroxyl ions (OH^-) ions increases in solutions and these ions have a higher attraction to the Uio-66 and ZIF-8 surface than CrO_4^{-2}. Because of the changing of chromium species (from $HCrO_4^-$ and $Cr_2O_7^{2-}$ to CrO_4^{-2}) and the presence of competitive ions (such as OH^-) under basic conditions, the chromium adsorption capacity was significantly reduced [4]. Of course, this decrease in the adsorption capacity in Uio-66 was higher because the pH_{ZPC} (≅7) is lower than that of ZIF-8 (≅9). At pH above the pH_{ZPC}, the charge on the surface of the adsorbents is negative. In this study, the best pH for removing chromium 7 was reported. Maximum adsorption of chromium has been achieved at the pH ≅ 3. As a result, the pH of 3 was selected for further experiments.

To study the effect of initial concentration, the chromium concentration of 10 to 200 mg/l was used. Figure 3 the effect of initial chromium concentration by Uio-66 and ZIF-8 adsorbents. At a constant pH, by increasing metal concentration, at first, the adsorption removal and capacity increased. In this study, the optimal concentration of chromium was found 10 mg/l. The different adsorption behaviour can be explained that with the increasing initial concentrations, the affinity of chromium molecules to adsorb on Uio-66 and ZIF-8 were increased (compared with lower concentrations) [42]. As a result, with increasing the concentrations of chromium, the adsorption capacity increased. After some time, the amount of chromium adsorption decreased. At low concentration, enough adsorption site onto Uio-66 and ZIF-8 surface are exist for chromium, and conversely [42]. As a result with an increase of the chromium concentration, adsorption was decreased. This fact can be explained by the mass transfer of Cr^{6+} and pressure onto the inner adsorption sites of the

Table 2 Calculated parameters of kinetic models for the chromium adsorption onto Uio-66 and ZIF-8

kinetics (Uio-66)	Parameters	Cr (VI) concentration (mg l^{-1})		Kinetics (ZIF-8)	Parameters	Cr (VI) concentration (mg l^{-1})	
		50	80			50	80
pseudo first order	k_1	0.0065	0.0111	pseudo first order	k_1	0.0065	0.0111
	R^2	0.663	0.689		R^2	0.7630	0.778
	q_{cal}	2.8730	20.9639		q_{cal}	2.8730	20.9639
pseudo second order	k_2	0.0566	0.0040	pseudo second order	k_2	0.0566	0.0040
	R^2	0.987	0.978		R^2	0.896	0.995
	$q_{e\ (cal)}$	27.6	54.6		$q_{e\ (cal)}$	58.6	120.6

Table 3 Calculated parameters of isotherm models for the chromium adsorption onto Uio-66 and ZIF-8

Isotherm (Uio-66)	Parameters	Cr (VI) concentration (mg l^{-1})		Isotherm (ZIF-8)	Parameters	Cr (VI) concentration (mg l^{-1})	
		50	80			50	80
Freundlich	n	3.45	4.56	Freundlich	n	2.42	3.78
	R^2	0.876	0.884		R^2	0.785	0.874
	K_F	20.12	21.34		K_F	23.4	23.7
Langmuir	K_L	1.675	1.243	Langmuir	K_L	0.876	0.985
	R^2	0.983	0.965		R^2	0.897	0.894
	q_m	35.78	85.45		q_m	76.65	150.85

adsorbent [13]. In lower concentrations, also, chromium molecules are adsorbed on Uio-66 and ZIF-8 adsorbent surface, rapidly, but with the increasing initial chromium concentration, gradually adsorbents surfaces become saturated. Finally, the adsorption decreased because of the repulsion between chromium molecules [43, 44]. The results of this study are consistent with the findings of other researchers [1].

Figure 4 shows the effect of Uio-66 and ZIF-8 dose and removal efficiency of chromium. It was observed that chromium adsorption increased with the increasing adsorbent dose until reaching an equilibrium dose. Equilibrium dosage for Uio-66 and ZIF-8 was 0.4 g/l and 0.6 g/l, respectively. In the following by increasing the adsorbent dose, chromium adsorption was not significant. Based on the results of another study, the increase of adsorption with adsorbent dose can be caused by high adsorbent surface and the availability of more adsorption sites [1]. At a higher dose than optimum (0.4 g/l and 0.6 g/l) by increasing than the dosage, the adsorption capacity of adsorbent was almost constant. The cause of that can be because of overlapping or aggregation of adsorption sites of adsorbents which finally lead to a decrease in the total surface area [1, 45]. The results of this study are consistent with the findings of other researchers. The findings of Mobarak et al. (2018) showed that dose increases from 0.05 to 2 mg, adsorption efficiency increases because of added sorption sites. However, increasing the dose does not have any effect on the adsorption efficiency [4].

Contact time is one of the leading factors determining the adsorption behaviour of a process [36]. To understanding the amount of chromium adsorbed onto adsorbents at various time, contact time was used. Figure 5 shows the effect of contact time on chromium adsorption onto Uio-66 and ZIF-8. Initially, chromium was adsorbed quickly onto Uio-66 and ZIF-8. Adsorption equilibrium was performed after 60 min and after this time, chromium adsorption did not significantly change. After this time (60 min), qe were nearly constant because of the saturation of active sites and the attainment of dynamic equilibrium step [4]. Table 2 shows calculated parameters of kinetic models for the Cr (VI) adsorption onto Uio-66 and ZIF-8. In order to choose the best kinetic model, the coefficient of determination (R^2) is checked. Actually, the agreement between the model predicted values and experimental data was determined by R^2 [41]. As illustrated in Table 2, the pseudo-second-order model for Uio-66 has the highest square R. As a result, this model was a fit model to describe the adsorption kinetics of chromium on Uio-66. Also for ZIF-8, pseudo-second-order model has the highest coefficient of determination (R^2). As a result, this model was a fit model to describe the adsorption kinetics of chromium on ZIF-8. So, it can be concluded that in the adsorption the rate-limiting step is mainly chemisorption which involves valence forces, occurred possibly because of exchange of electrons among chromium and adsorbents [41]. The present results showed which chromium adsorption onto Uio-66 and ZIF-8 was very fast and more than 95% of the equilibrium adsorption capacity was

Table 4 Comparison of the chromium adsorption capacity onto Uio-66 and ZIF-8 with other adsorbents

Adsorbent	qe (mg g^{-1})	Reference
Cu-TBC	48	[1]
ZIF-67	15.43	[11]
treated waste newspaper	59.88	[46]
Novel Diazene/Methoxy-Laced Coordination Polymer	106.13	[36]
sliver-triazolate MOF	38.6	[14]
CTAB/H_2O_2	67.05	[4]
Mesoporous carbon microspheres (MCMs)	156.3	[41]
Carbon nano-onions (CNOs)	23.527 (pH ≈ 7), 27.855 (pH ≈ 3)	[47]
GnZVI/PAC	53.48	[37]
Uio-66	85.7	(This study)
ZIF-8	150	(This study)

achieved in the first 60 min. The equilibrium time of Uio-66 and ZIF-8 for chromium adsorption was approximately 350 min (5.83 h), respectively. Table 3 shows the calculated parameters of isotherm models for the chromium adsorption onto Uio-66 and ZIF-8. As shown in Table 3, the Langmuir isotherm model has the most coefficient of determination, so, chromium adsorption onto both Uio-66 and ZIF-8 conform to the model. The Langmuir model suggests monolayer adsorption process and the homogeneous surface of adsorbent which indicates that active sites of chromium adsorption have been distributed throughout the surface of adsorbents [41]. According to this model, the maximum of chromium adsorption capacity for Uio-66 and ZIF-8 was 85.7 mg/g and 150 mg/g, respectively. As is clear, the two parameters surface area and pore volume have a significant impact on the amount of pollutant adsorption. The adsorption capacity varies and depends mainly on the initial chromium concentration and characteristics of the individual adsorbent [41]. Maleki et al. (2015) reported that the maximum adsorption capacity of chromium on Cu-BTC is on activated carbon adsorbent 48 mg/g [1]. Table 4 shows a comparison of the adsorption chromium capacity onto Uio-66 and ZIF-8 with other adsorbents. According to Table 4, the adsorption chromium capacity ZIF-8 is significantly more than that of other adsorbents.

Conclusion

In this study, metal organic frameworks of Uio-66 and ZIF-8 were synthesized based on previous works. Chromium adsorption was dependent on adsorbent dose, solution pH, and initial concentration, and contact time. The residual chromium concentration at 540 nm was determined using a spectrophotometer (UV-UVIS). The rate of chromium adsorption was higher under acidic conditions. pH_{ZPC} for Uio-66 and ZIF-8 was obtained 7 and 9, respectively. The findings of this study showed that chromium adsorption capacity in ZIF-8 (150 mg/g) was higher than Uio-66 (85.6 mg/g) at an initial concentration of 50 mg/*L. maximum* adsorption of chromium has been achieved at the pH ≅ 3. One of the reasons for higher adsorption of chromium in ZIF-8 (1050 m^2/g) can be a higher surface area than Uio-66 (800 m^2/g). In this study, the optimal concentration of chromium was found 10 mg/l. The equilibrium time of chromium adsorption onto Uio-66 and ZIF-8 was approximately 350 min. The findings of the study showed that the experimental data obtained fitted with kinetic model pseudo-order- reaction and isotherm model of Langmuir.

Acknowledgements The authors of the research thanks Lorestan University of Medical Sciences to support research (NO. 140).

Author contribution KM Thabayneh distributed, collected and read the dosimeters, analyzed, wrote the text, reviewed and approved the final manuscript.

Compliance with ethical standards

Ethics approval and consent to participate Not applicable.

Consent for publication Not applicable.

Competing interests The author declares that they have no competing interests.

References

1. Maleki A, Hayati B, Naghizadeh M, Joo SW. Adsorption of hexavalent chromium by metal organic frameworks from aqueous solution. J Ind Eng Chem. 2015;28:211–6.
2. Shirzad SM, Azizian S, Maleki A, Zarrabi M. Removal of chromium by using of adsorption onto strong base anion resin: study of equilibrium and kinetic. Water & wastewater. 2011:10–8.
3. Anirudhan T, Raji C. Choromium (VI) adsorption by sawdust carbon: kinetics and equilibrium [J]. Indian Journal of Chemical Technology. 1997;4:228–36.
4. Mobarak M, Selim AQ, Mohamed EA, Seliem MK. A superior adsorbent of CTAB/H_2O_2 solution-modified organic carbon rich-clay for hexavalent chromium and methyl orange uptake from solutions. J Mol Liq. 2018;259:384–97.
5. Siboni MS, Samadi M, Azizian S, Maleki A, Zarrabi M. Removal of chromium by using of adsorption onto strong base anion resin: study of equilibrium and kinetic. Water Wastewater. 2011;3:10–8.
6. Entezari A, Khosravi R, Arghavan FA, Taghizadeh A, Khodadadi M, Eslami H. Investigation of hexavalent chromium removal from aqueous solution using granular and powdered activated carbon produced from peganum harmala seed. 2016 J Rafsanjan Univ Med Sci. 2016;15:645–56.
7. Panda H, Tiadi N, Mohanty M, Mohanty C. Studies on adsorption behavior of an industrial waste for removal of chromium from aqueous solution. South African Journal Of Chemical Engineering. 2017;23:132–8.
8. Hu J, Chen G, Lo IM. Removal and recovery of Cr (VI) from wastewater by maghemite nanoparticles. Water Res. 2005;39:4528–36.
9. Gopal Reddi MR, Gomathi T, Saranya M, Sudha PN. Adsorption and kinetic studies on the removal of chromium andcopper onto chitosan-g-maliec anhydride-g-ethylene dimethacrylate. Int J Biol Macromol. 2017;104:1578–85.
10. Mohsenibandpei A, Alinejad A, Bahrami H, Ghaderpoori M. Water solution polishing of nitrate using potassium permanganate modified zeolite: parametric experiments, kinetics and equilibrium analysis. Global Nest Journal. 2016;18:546–58.
11. Li X, Gao X, Ai L, Jiang J. Mechanistic insight into the interaction and adsorption of Cr (VI) with zeolitic imidazolate framework-67 microcrystals from aqueous solution. Chem Eng J. 2015;274:238–46.
12. Shen L, Liang S, Wu W, Liang R, Wu L. Multifunctional NH_2-mediated zirconium metal–organic framework as an efficient visible-light-driven photocatalyst for selective oxidation of alcohols and reduction of aqueous Cr(VI)†. Dalton Trans. 2013;42:13649–57.
13. Vala RM, Wankasi D, Dikio ED. Morphology and adsorption of chromium ion on uranium 1, 2, 4, 5-benzenetetracarboxylic acid metal organic framework (MOF). Hemijska industrija. 2016;70:565–72.
14. Li LL, Feng XQ, Han RP, Zang SQ, Yang G. Cr (VI) removal via anion exchange on a silver-triazolate MOF. J Hazard Mater. 2017;321:622–8.
15. Huo SH, Yan XP. Metal–organic framework MIL-100(Fe) for the adsorption of malachite green from aqueous solution. J Mater Chem. 2012;22:7449–55.

16. Ghaderpoori M. Metal organic framework Uio-66 for adsorption of methylene blue dye from aqueous solutions. Int J Environ Sci Technol. 2017;14:1959–68.
17. Zhou M, Wu YN, Qiao J, Zhang J, McDonald A, Li G, et al. The removal of bisphenol a from aqueous solutions by MIL-53(Al) and mesostructured MIL-53(Al). J Colloid Interface Sci. 2013;405: 157–63.
18. Seo YS, Khan NA, Jhung SH. Adsorptive removal of methylchlorophenoxypropionic acid from water with a metal-organic framework. Chem Eng J. 2015;270:22–7.
19. Liu B, Jian M, Liu R, Yao J, Zhang X. Highly efficient removal of arsenic (III) from aqueous solution by zeolitic imidazolate frameworks with different morphology. Colloids Surf A Physicochem Eng Asp. 2015;481:358–66.
20. Luu CL, Nguyen TTV, Nguyen T, Hoang TC. Synthesis, characterization and adsorption ability of UiO-66-NH_2. Adv Nat Sci Nanosci Nanotechnol. 2015;6:1–7.
21. Shen L, Wu W, Liang R, Lin R, Wu L. Highly dispersed palladium nanoparticles anchored on UiO-66(NH_2) metal-organic framework as a reusable and dual functional visible-lightdriven photocatalyst. The Royal Society of Chemistry. 2013;5.19:9374–82.
22. Furukawa H, Cordova KE, O'Keeffe M, Yaghi OM. The chemistry and applications of metal-organic frameworks. Science. 2013;341: 1230444– to 12.
23. Eaton AD, Clesceri LS, EW R. Standard methods for the xamination of water and wastewater (PAHA). Washington DC, USA: American Water Works Association; 2005.
24. Cai HM, Chen GJ, Peng CY, Zhang ZZ, Dong YY, Shang GZ, et al. Removal of fluoride from drinking water using tea waste loaded with Al/Fe oxides: a novel, safe and efficient biosorbent. Appl Surf Sci. 2015;328:34–44.
25. Golmohammadi S, Ahmadpour M, Mohammadi A, Alinejad A, Mirzaei N, Ghaderpoori M, et al. Removal of blue cat 41 dye from aqueous solutions with ZnO nanoparticles in combination with US and US-H2O2 advanced oxidation processes. Environmental Health Engineering and Management Journal. 2016;3:107–13.
26. Mohammadi AA, Alinejad A, Kamarehie B, Javan S, Ghaderpoury A, Ahmadpour M, et al. Metal-organic framework Uio-66 for adsorption of methylene blue dye from aqueous solutions. Int J Environ Sci Technol. 2017:1–10.
27. Reardon EJ, Wang Y. A limestone reactor for fluoride removal from wastewaters. Environ Sci Technol. 2000;34:3247–53.
28. Bhaumik R, Mondal NK, Chattoraj S, Datta JK. Application of response surface methodology for optimization of fluoride removal mechanism by Newely developed biomaterial. Am J Anal Chem. 2013;4:404–19.
29. Massoudinejad M, Ghaderpoori M, Shahsavani A, Amini MM. Adsorption of fluoride over a metal organic framework Uio-66 functionalized with amine groups and optimization with response surface methodology. J Mol Liq. 2016;221:279–86.
30. Peterson GW, DeCoste JB, Fatollahi-Fard F, Britt DK. Engineering UiO-66-NH_2 for toxic gas removal. Ind Eng Chem Res. 2014;53: 701–7.
31. Lin L, Zhai SR, Xiao ZY, Song Y, An QD, Song XW. Dye adsorption of mesoporous activated carbons produced from NaOH-pretreated rice husks. Bioresour Technol. 2013;136:437–43.
32. Lin KYA, Chen SY, Jochems AP. Zirconium-based metal organic frameworks: highly selective adsorbents for removal of phosphate from water and urine. Mater Chem Phys. 2015;160:168–76.
33. Nordin NAHM, Racha SM, Matsuura T, Misdan N, Sani NAA, Ismail AF, et al. Facile modification of ZIF-8 mixed matrix membrane for CO_2/CH_4 separation: synthesis and preparation. RSC Adv. 2015;5(54):43110–20.
34. Jian M, Liu B, Zhang G, Liu R, Zhang X. Adsorptive removal of arsenic from aqueous solution by zeolitic imidazolate framework-8 (ZIF-8) nanoparticles. Colloids Surf A Physicochem Eng Asp. 2015;465:67–76.
35. Khan NA, Jung BK. Hasan Z, Jhung SH. Adsorption and removal of phthalic acid and diethyl phthalate fromwater with zeolitic imidazolate and metal–organic frameworks. J Hazard Mater. 2015;282:194–200.
36. Liu LL, Xing Y, Yu HY, Zhang CW, Ye MQ, Miao MZ, et al. Effective removal of chromium (III) from low concentration aqueous solution using a novel Diazene/Methoxy-laced coordination polymer. Polymers. 2017;9:273.
37. Khosravi R, Moussavi G, Ghaneian MT, Ehrampoush MH, Barikbin B, Ebrahimi AA, et al. Chromium adsorption from aqueous solution using novel green nanocomposite: adsorbent characterization, isotherm, kinetic and thermodynamic investigation. J Mol Liq. 2018;256:163–74.
38. Massoudinejad M, Ghaderpoori M, Shahsavani A, Jafari A, Kamarehie B, Ghaderpoury A, et al. Ethylenediamine-functionalized cubic ZIF-8 for arsenic adsorption from aqueous solution: modeling, isotherms, kinetics and thermodynamics. J Mol Liq. 2018;255:263–8.
39. Chen JH, Xing HT, Guo HX, Weng W, Hu SR, Li SX, et al. Investigation on the adsorption properties of Cr(vi) ions on a novel graphene oxide (GO) based composite adsorbent. J Mater Chem A. 2014;2:12561–70.
40. Zhang S, Li J, Wen T, Xu J, Wang X. Magnetic Fe_3O_4@NiO hierarchical structures: preparation and their excellent as(v) and Cr(vi) removal capabilities. RSC Adv. 2013;3:2754–64.
41. Zhou J, Wang Y, Wang J, Qiao W, Long D, Ling L. Effective removal of hexavalent chromium from aqueous solutions by adsorption on mesoporous carbon microspheres. J Colloid Interface Sci. 2016;462:200–7.
42. Qin Q, Wang Q, Fu D, Ma J. An efficient approach for Pb(II) and cd(II) removal using manganese dioxide formed in situ. Chem Eng J. 2011;172:68–74.
43. García ER, Medina RL, Lozano MM, Pérez IH, Valero MJ, Franco AMM. Adsorption of azo-dye Orange II from aqueous solutions using a metal-organic framework material: Iron-Benzenetricarboxylate. Materials. 2014;7:8037–57.
44. Zvinowanda CM, Okonkwo JO, Sekhula MM, Agyei NM, Sadiku R. Application of maize tassel for the removal of Pb, se, Sr, U and V from borehole water contaminated with mine wastewater in the presence of alkaline metals. J Hazard Mater. 2009;164:884–91.
45. Zhang N, Yang X, Yu X, Jia Y, Wang J, Kong L, et al. Al-1,3,5-benzenetricarboxylic metal–organic frameworks: a promising adsorbent for defluoridation of water with pH insensitivity and low aluminum residual. Chem Eng J. 2014;252:220–9.
46. Dehghani MH, Sanaei D, Ali I, Bhatnagar A. Removal of chromium (VI) from aqueous solution using treated waste newspaper as a low-cost adsorbent: kinetic modeling and isotherm studies. J Mol Liq. 2016;215:671–9.
47. Sakulthaew C, Chokejaroenrat C, Poapolathep A, Satapanajaru T, Poapolathep S. Hexavalent chromium adsorption from aqueous solution using carbon nano-onions (CNOs). Chemosphere. 2017;184: 1168–74.